Thermodynamically Explicit Kinetics with Potential for Genome-wide Application

March 2, 2025

Oliver Bodeit[1,†], Chalermroj Sutthaphirom[2,†], Rune Linding[1], Pimchai Chaiyen[2], and Edda Klipp[1,*]

[1]Klipp-Linding Lab, Theoretical Biophysics, Humboldt-Universität zu Berlin, Invalidenstr. 42, 10115 Berlin,Germany
[2]Vidyasirimedhi Institute of Science and Technology (VISTEC), Wangchan Valley, 555 Moo 1 Payupnai, Wangchan, Rayong 21210 Thailand

Correspondence: edda.klipp@rz.hu-berlin.de
[†]These authors contributed equally to this work.

Abstract

Metabolic processes are fundamental to life, and understanding their dynamic behavior is crucial for addressing biological questions and advancing applications in medicine and biotechnology. While genome-scale metabolic network reconstructions and constraint-based modeling, such as Flux Balance Analysis (FBA), have provided valuable insights into steady-state metabolism, their inherent limitations in capturing dynamic behavior restrict our ability to predict and manipulate metabolic responses, particularly in complex scenarios like disease. This is especially critical for understanding and treating conditions like cancer. This work addresses this challenge by developing a thermodynamically explicit (TDE) parametrization of kinetic models for metabolic reaction systems, grounded in the principles of equilibrium and non-equilibrium thermodynamics. Specifically, we (1) revisit classical kinetic modeling approaches using Michaelis-Menten and convenience kinetics, (2) leverage thermodynamic principles to derive a TDE parametrization method, and (3) demonstrate the impact of TDE parametrization by comparing simulations of a realistic metabolic model using both classical and TDE approaches. We anticipate that this TDE kinetic approach will be a valuable tool for genome-scale parametrization of dynamic metabolic network models, enabling more accurate and predictive simulations of metabolic behavior under diverse conditions.

1 Introduction

1.1 Mathematical Modeling of Metabolism: From Steady-State to Dynamic Approaches

Metabolism is crucial to all life, and understanding its complexities is vital for various biological applications. Here, we focus on metabolic dynamics aiming to bridge the gap between steady-state and dynamic models. While genome-scale metabolic network reconstructions and constraint-based modeling like Flux Balance Analysis (FBA) have advanced our understanding of steady-state metabolic fluxes, their inherent limitation in capturing the dynamic nature of metabolic processes hinders our ability to predict and control metabolic behavior under changing conditions, especially in disease states like cancer.

Life depends on energy exchange, governed by the fundamental laws of thermodynamics. These laws are essential for comprehending the potential and limitations of cellular growth and metabolism. Systems biology utilizes mathematical models to describe cellular processes, but their predictive power relies on adhering to these fundamental physical and chemical laws, particularly thermodynamics. Life is inherently dynamic across all scales. Mathematical models explain observed behaviors in diverse biological processes, including metabolism. Notably, many metabolic phenomena can be explained

by steady-state models, forming the basis of FBA and related approaches. However, these methods neglect temporal dynamics and quantitative values of metabolite concentrations, both crucial for understanding biological systems. Non-equilibrium thermodynamics provides the framework to address time-dependent processes, determine directionality, and quantify energy expenditure associated with dynamic trajectories.

1.2 Introducing Thermodynamically Explicit (TDE) Kinetics: A Novel Approach

To bridge the gap between steady-state and dynamic models, we propose integrating thermodynamic principles into kinetic models for enzymatic reactions. We present a Thermodynamically Explicit (TDE) framework to transform existing FBA models into dynamic and quantitative models of metabolism. This approach aims to be mathematically robust, computationally tractable, and widely applicable. TDE kinetics offers mathematical correctness, simplicity in obtaining or estimating parameters compared to classical kinetics, and utility in parametrization of large metabolic networks.

In this work, we will first revisit fundamental principles starting with phenomenological equilibrium thermodynamics, progressing to open systems, steady states, and deviations. On this basis, we will, second, introduce the concept of TDE kinetics and the relevant mathematical formulations. Third, we will apply the approach to an established, carefully parameterized model of glycolysis in order to demonstrate the practical application and also the challenges coming with the new approach. Eventually, this research aims to develop a novel, thermodynamically grounded approach to model metabolic dynamics, enhancing our understanding and predictive capabilities beyond the limitations of current steady-state methods. We foresee that applications will include biotechnological processes, such as chemostat and batch cultures, as well as the metabolic shifts observed between healthy and cancerous cells.

2 Fundamental Principles of Reaction Kinetics

2.1 The Law of Mass Action and Classical Kinetics

For the classical description of the dynamics of metabolic networks, a number of kinetic rate laws have been introduced. With a few exceptions, they are all based on the law of mass action introduced already in the 1860s by Guldberg and Waage [GW67, WG64]. This law states that a reaction rate v is proportional to the rate of collision of the reactants which, in turn, is proportional to their concentration to the power of the molecularity with which they enter the reaction. Exemplified for the following reaction

$$A+B \underset{k_-}{\overset{k_+}{\rightleftharpoons}} 2C$$

the reaction rate would read

$$v = v_+ - v_- = A \cdot B \cdot k_+ - C^2 \cdot k_-, \tag{1}$$

where A, B, and C also denote the concentrations of A, B, and C, resp., and k_+ and k_- are the forward and backward kinetic constants, respectively.

For enzyme catalyzed reactions, binding of substrate S to the enzyme E to form an enzyme-substrate complex ES and the release of the product P are considered as two different processes. For the irreversible case, the reaction scheme looks as follows

$$E+S \underset{k_{-1}}{\overset{k_{+1}}{\rightleftharpoons}} ES \xrightarrow{k_{+2}} E+P$$

and the rate equation (Michaelis-Menten rate equation, [MM+13]) reads

$$v = \frac{E_{total} \cdot k_{+2} \cdot S}{\frac{k_{-1}+k_{+2}}{k_{+1}} + S} = \frac{V_{max} \cdot S}{K_M + S}, \tag{2}$$

where S denotes the concentration of the substrate, $V_{max} = E_{total} \cdot k_{+2}$ is the maximum rate of this reaction and $K_M = \frac{k_{-1}+k_{+2}}{k_{+1}}$ is the Michaelis-Menten constant.

For the reversible case, the reaction scheme changes slightly:

$$E{+}S \underset{k_{-1}}{\overset{k_{+1}}{\rightleftharpoons}} ES \underset{k_{-2}}{\overset{k_{+2}}{\rightleftharpoons}} E{+}P$$

leading to the following rate equation

$$v = E_{total} \frac{k_{+1} \cdot k_{+2} \cdot S - k_{-1} \cdot k_{-2} \cdot P}{k_{+1} \cdot S + k_{-1} + k_{+2} + k_{-2} \cdot P} = \frac{\frac{V^f_{max}}{K_{MS}} \cdot S - \frac{V^b_{max}}{K_{MP}} \cdot P}{1 + \frac{S}{K_{MS}} + \frac{P}{K_{MP}}}, \tag{3}$$

Here, V^f_{max} and V^b_{max} denote the maximal rates of forward and backward reactions, resp., while K_{MS} and K_{MP} are the Michaelis-Menten constants of substrate and product, resp., in this reaction.

The kinetic constants obey a relation to the equilibrium constant q of the reaction, it holds

$$q = \frac{k_{+1} \cdot k_{+2}}{k_{-1} \cdot k_{-2}} = \frac{V^f_{max} \cdot K_{MP}}{V^b_{max} \cdot K_{MS}}, \tag{4}$$

A number of various rate equations have been introduced that take different mechanisms for inhibition, ligand binding or cooperativity into account. For reactions with two or more substrates there are, for example, ordered bi-bi mechanism, ping-pong kinetics, random kinetics. To simplify and generalize these various kinetics, we introduced the so-called convenience kinetics [LK06], which is now frequently used especially in computational approaches. To this end, we normalize all concentration values by the specific Michaelis-Menten constant of this compound in the reaction, i.e.

$$\tilde{s} = \frac{S}{K_{MS}}, \quad \tilde{p} = \frac{P}{K_{MP}} \tag{5}$$

or, in general, for substrates S_i with $i = 1...n$ in reaction r

$$\tilde{s_i} = \frac{S_i}{K_{MS_{i,r}}} \tag{6}$$

We also consider that V^f_{max} and V^b_{max} can be written as $E \cdot k^f_{cat}$ and $E \cdot k^b_{cat}$, respectively. With this, the convenience kinetics for a reaction with one substrate and product reads

$$v = E_{total} \frac{k^f_{cat} \cdot \tilde{s} - k^b_{cat} \cdot \tilde{p}}{1 + \tilde{s} + 1 + \tilde{p} - 1}, \tag{7}$$

and for a reaction with n substrates and m products

$$v = E_{total} \frac{k^f_{cat} \cdot \prod_{i=1}^{n} \tilde{s_i} - k^b_{cat} \cdot \prod_{j=1}^{m} \tilde{p_j}}{\prod_{i=1}^{n}(\tilde{s_i} + 1) + \prod_{j=1}^{m}(\tilde{p_j} + 1) - 1}, \tag{8}$$

2.2 Stoichiometry

In biochemical reaction networks with R reactions and K reactants, reactants can undergo different reactions at the same time. This is typically expressed by balance equations for their concentration changes either separately as

$$\frac{\mathrm{d}S_i}{\mathrm{d}t} = \sum_{r}^{R} (n_{ir} v_r) \tag{9}$$

for the i-th compound or in matrix form as

$$\frac{\mathrm{d}\vec{S}}{\mathrm{d}t} = \mathbf{N}\vec{v} \tag{10}$$

where

$$\mathbf{N} = \begin{bmatrix} n_{11} & n_{12} & \dots & n_{1R} \\ n_{11} & n_{12} & \dots & n_{1R} \\ & & \ddots & \\ n_{K1} & n_{K2} & \dots & n_{KR} \end{bmatrix} \tag{11}$$

is the stoichiometric matrix of the reaction system.

3 Thermodynamically Explicit Kinetic Constants

3.1 Thermodynamically Explicit Kinetics of Individual Reactions

Let's consider a monomolecular reaction r with one substrate, S_i, and one product, S_j.

$$S_i \underset{k_{-r}}{\overset{k_{+r}}{\rightleftharpoons}} S_j$$

where k_{+r} and k_{-r} are the forward and backward kinetic constants, respectively. Be it further assumed that all reaction rates v follow mass action kinetics (i.e. $v_{+r} = S_i \cdot k_{+r}$). Then, the reaction rate reads

$$v_r = v_{+r} - v_{-r} = S_i \cdot k_{+r} - S_j \cdot k_{-r}, \tag{12}$$

where S_i and S_j also denote the concentrations of S_i and S_j, resp.. The chemical affinity A_r of the reaction is defined as

$$A_r = \mu_i - \mu_j = \mu_i^0 + RT \ln S_i - \mu_j^0 - RT \ln S_j, \tag{13}$$

with $\mu_{i,j}$ being the chemical potential of compounds $S_{i,j}$ and $\mu_{i,j}^0$ its standard chemical potential, respectively. R is the gas constant and T temperature. Note that under standard conditions (all concentrations measured in 1 M), the affinity A_r equals the Gibbs free energy $\Delta_r G'^{\circ}$ as also discussed below in the application. At equilibrium, both affinity and reaction rate vanish, i.e. it holds that $A_r = 0$ and, thus,

$$\mu_i^0 + RT \ln S_i = \mu_j^0 + RT \ln S_j. \tag{14}$$

Rearranging of (14), while considering that also $v_r = 0$ at equilibrium, results in

$$e^{\frac{\mu_i^0 - \mu_j^0}{RT}} = \frac{S_j}{S_i}|_{eq} = \frac{k_{+r}}{k_{-r}}. \tag{15}$$

Equation (15) provides us with a relation between the rate constants $k_{\pm r}$ and the chemical standard potentials μ^0,

$$k_{+r} = \lambda_r e^{\frac{\mu_i^0}{RT}}, \qquad k_{-r} = \lambda_r e^{\frac{\mu_j^0}{RT}} \tag{16}$$

with a yet undefined parameter λ_r. Since both the chemical standard potentials and the kinetic constants are constants, this relationship holds also away from the equilibrium (although we derived it for the equilibrium). The parameter λ_r results from the fact that for the reaction rate only the difference in chemical potentials of the reactants matters, not their absolute values. λ_r can be interpreted as being related to the height of the activation energy along the reaction coordinate and is dependent on both the amount and the activity of the catalyzing enzyme. Note that the transition from Equation (15) to Equation (16) is not unambiguous in the mathematical sense, meaning that with Equation (16) also $k_{+r} = \lambda_r^* \exp \frac{\mu_i^0 + \beta}{RT}$ and $k_{-r} = \lambda_r^* \exp \frac{\mu_j^0 + \beta}{RT}$ with $\lambda_r^* = \lambda_r \exp \frac{-\beta}{RT}$ for every real number β would also be a valid solution. We will use this fact in the application below.

Introducing expression (16) into the general rate equation (12), the reaction rate v_r reads

$$v_r = \lambda_r (S_i e^{\frac{\mu_i^0}{RT}} - S_j e^{\frac{\mu_j^0}{RT}}) \tag{17}$$

The expressions for reaction rate, affinity and kinetic constants introduced here will now be extended for biochemical reaction networks.

3.2 Thermodynamically Explicit Kinetic Constants in Reaction Networks

For the purpose of relating kinetic parameters of individual reactions to the network stoichiometry, we will below separate the stoichiometric matrix given in Equation (11) into a producing part and a degrading part

$$\mathbf{N} = \mathbf{N}_+ + \mathbf{N}_-, \tag{18}$$

where $\mathbf{N}_+$ comprises only stoichiometric coefficients for the production of reactants and $\mathbf{N}_-$ only for the degrading contributions. Below, they will together be called the partial stoichiometric matrices. We use

$$\mathbf{N}_\pm = \begin{cases} n_{ir}, \text{ if } \pm\, n_{ir} > 0 \\ 0, \text{ otherwise} \end{cases} \tag{19}$$

Let's consider an example. For the following network consisting of three reactants and two monomolecular reactions

$$S_1 \underset{k_{-1}}{\overset{k_{+1}}{\rightleftharpoons}} S_2 \underset{k_{-2}}{\overset{k_{+2}}{\rightleftharpoons}} S_3$$

the full stoichiometric matrix as well as its degrading and producing parts read

$$\mathbf{N} = \begin{bmatrix} -1 & 0 \\ 1 & -1 \\ 0 & 1 \end{bmatrix} \quad \mathbf{N}_- = \begin{bmatrix} -1 & 0 \\ 0 & -1 \\ 0 & 0 \end{bmatrix} \quad \mathbf{N}_+ = \begin{bmatrix} 0 & 0 \\ 1 & 0 \\ 0 & 1 \end{bmatrix} \tag{20}$$

Next, we create two new vectors, $\vec{M}_\pm$, by multiplication of the vector containing the standard chemical potentials, i.e. $\vec{\mu}_0 = [\mu_1, \mu_2, ..., \mu_K]^{\mathrm{T}}$ with the partial stoichiometric matrices, i.e.

$$\vec{M}_\pm = \vec{\mu}_0^{\mathrm{T}} \cdot \mathbf{N}_\pm \tag{21}$$

Here, the superscript T denotes the transpose of the vector (i.e. switch between a row and a column vector). Then, the kinetic constants of the r-th reaction read as follows

$$k_{\pm r} = \lambda_r e^{\mp \frac{M_{\mp r}}{RT}} \tag{22}$$

where $M_{\pm r}$ is the r-th entry of $\vec{M}_\pm$.

For the above example (two successive monomolecular reactions), these quantities read

$$\vec{M}_- = \begin{bmatrix} \mu_1^0 & \mu_2^0 & \mu_3^0 \end{bmatrix} \cdot \begin{bmatrix} -1 & 0 \\ 0 & -1 \\ 0 & 0 \end{bmatrix} = \begin{bmatrix} -\mu_1^0 & -\mu_2^0 \end{bmatrix}$$

$$\vec{M}_+ = \begin{bmatrix} \mu_1^0 & \mu_2^0 & \mu_3^0 \end{bmatrix} \cdot \begin{bmatrix} 0 & 0 \\ 1 & 0 \\ 0 & 1 \end{bmatrix} = \begin{bmatrix} \mu_2^0 & \mu_3^0 \end{bmatrix}$$

and

$$k_{+1} = \lambda_1 e^{\frac{\mu_1^0}{RT}} \qquad k_{-1} = \lambda_1 e^{\frac{\mu_2^0}{RT}}$$

$$k_{+2} = \lambda_2 e^{\frac{\mu_2^0}{RT}} \qquad k_{-2} = \lambda_2 e^{\frac{\mu_3^0}{RT}}$$

For a bimolecular reaction, exemplified by the following reaction scheme,

$$S_1 + S_2 \underset{k_{-1}}{\overset{k_{+1}}{\rightleftharpoons}} S_3$$

with the following set of stoichiometric matrices

$$\mathbf{N} = \begin{bmatrix} -1 \\ -1 \\ 1 \end{bmatrix} \quad \mathbf{N}_+ = \begin{bmatrix} 0 \\ 0 \\ 1 \end{bmatrix} \quad \mathbf{N}_- = \begin{bmatrix} -1 \\ -1 \\ 0 \end{bmatrix} \tag{23}$$

we would obtain the affinity

$$A_1 = \mu_1 + \mu_2 - \mu_3 = \mu_1^0 + RT \ln S_1 + \mu_2^0 + RT \ln S_2 - \mu_3^0 - RT \ln S_3. \tag{24}$$

The equilibrium condition, with $S_1, S_2 \geq 0$, then reads

$$e^{\frac{\mu_1^0 + \mu_2^0 - \mu_3^0}{RT}} = \frac{S_3}{S_1 S_2}|_{eq} = \frac{k_{+1}}{k_{-1}}. \tag{25}$$

The $\vec{M}$-vectors have only one entry each and read

$$\vec{M}_{+1} = \left[\mu_3^0\right]$$
$$\vec{M}_{-1} = \left[-\mu_1^0 - \mu_2^0\right]$$

Consequently, the kinetic constants for this reactions are given by

$$k_{+1} = \lambda_1 e^{\frac{\mu_1^0 + \mu_2^0}{RT}}, \;\; k_{-1} = \lambda_1 e^{\frac{\mu_3^0}{RT}} \tag{26}$$

We note that all standard chemical potentials of the substrate enter a sum in the first exponential function. The same would hold for products and the second exponential, if there would be more than one product.

3.3 Reaction Rates for Networks with only Monomolecular Reactions

In order to simplify the representation of reaction rates of a network in condensed form, we introduce the following abbreviation for the product of reactant concentration and the exponential of its standard chemical potential devided by RT as

$$X_i = S_i e^{\frac{\mu_i^0}{RT}} \quad \text{for} \quad i = 1, ...K \tag{27}$$

Using 27, the rate of a monomolecular reaction reversible converting S_i into S_j given in 17 reads

$$v_r = \lambda_r (X_i - X_j) \quad \text{for} \quad r = 1, ...R \tag{28}$$

For a reaction network with the stoichiometric matrix $\mathbf{N}$ the vector of reaction rates, $\vec{v}$ can be expressed as follows

$$\vec{v}^{\mathrm{T}} = -\begin{bmatrix} X_1 & X_2 & ... & X_K \end{bmatrix} \cdot \begin{bmatrix} n_{11} & n_{12} & ... & n_{1R} \\ n_{11} & n_{12} & ... & n_{1R} \\ & & \ddots & \\ n_{K1} & n_{K2} & ... & n_{KR} \end{bmatrix} \cdot \begin{bmatrix} \lambda_1 & 0 & ... & 0 \\ 0 & \lambda_2 & ... & 0 \\ & & \ddots & \\ 0 & 0 & ... & \lambda_R \end{bmatrix} \tag{29}$$

or

$$\vec{v} = -[\vec{X}^{\mathrm{T}} \mathbf{N} Diag(\lambda)]^{\mathrm{T}} \tag{30}$$

$Diag(\lambda)$ denotes the $R \times R$ diagonal matrix containing the λ values in its main diagonal.
In steady state, we have

$$\mathbf{N}\vec{v} = 0 \tag{31}$$

Introducing the vector for rates from (30) gives

$$\mathbf{N}[\vec{X}^{\mathrm{T}} \mathbf{N} Diag(\lambda)]^{\mathrm{T}} = 0 \tag{32}$$

Rearranging yields

$$\mathbf{N} Diag(\lambda) \mathbf{N}^{\mathrm{T}} \vec{X} = 0 \tag{33}$$

This is a homogeneous linear equation system, which could be solved either for the values of $\vec{\lambda}$ (i.e. the contribution of enzyme activities to rates) if $\vec{X}$ (i.e. the concentrations and standard chemical potentials of reactants) is given, or for the values of $\vec{X}$ if $\vec{\lambda}$ is given.

4 Proof of Principle: Application of TDE Kinetics to a Model of Glycolysis (Hynne model)

In order to demonstrate that the suggested kinetics is applicable to metabolic networks, we used an introduced and frequently used model of central carbon metabolism in yeast, the Hynne model [HDS01]. It was developed to explain oscillatory behavior after addition of cyanide. It contains 22 metabolites and 24 metabolic reactions, the kinetics and parameter values of which have been carefully extracted from literature and adapted to experimental data.

In applying the TDE kinetics to this model, now considered as ground truth, a series of practical problems have to be solved and technical considerations have to be taken. First, we need to obtain values for the standard chemical potentials for all represented metabolites and ensure that all model compounds are used in the appropriate physical units. Second, we have to revisit the stoichiometric matrix to ensure that all thermodynamically relevant metabolites are appropriately represented and that explicit and implicit model assumptions (e.g. constant values for external metabolites) are taken into account. Third, we have to estimate the values of prefactors $\vec{\lambda}$. And eventually, we have to test in simulations that the resulting new model shows comparable dynamics to the original model.

To guide the reader's imaging about the model used, we provide a scheme of the reaction network containing both the original version and our additions (as discussed below) in Fig. 1. More information about the model can also be retrieved from the JWS online database [PEVN+17] containing implemented and simulatable models of many metabolic and other networks under https://jjj.mib.ac.uk/models/hynne/simulate/.

4.1 Values of Standard Chemical Potentials

The network-based parametrization of metabolic reactions requires two types of parameters: the standard chemical potentials μ_i^0 of each metabolite and the prefactors λ_r for each reaction. While classical chemical and biochemical literature provides numerous Gibbs energies for the reactions some standard chemical potentials (often calculated from formation enthalpies), a systematically collected and inherently coherent set of values is needed. Critically and as discussed above, all rates depend on *differences* of standard chemical potentials, not on absolute values.

To obtain a potentially genome-wide collection of standard chemical potentials, we used the publicly available tool eQuilibrator [BGM+22]. This tool employs a group contribution method [Alb94, Alb03, Mav91, NHMF13] to calculate reaction free energies, providing coherent values for user-selectable physical conditions like pH value and ionic strength. It also offers a comprehensive explanation of relevant thermodynamic terms (e.g. Gibbs free energy of reactions, Gibbs energy of formation, standard conditions), which we briefly summarize it here, aligning it with our notation.

"Standard conditions" imply all substrates and products are at 1 M concentration, denoted by a degree symbol "°" as in $\Delta_r G'^{\circ}$ for the Gibbs free energy of the r-th reaction. Standard conditions serve as reference point, as reactions rarely take place under these conditions. Concentration changes within the reaction system affect $\Delta_r G'$, which represents our concentration dependent affinity A_r. Realistic biological concentrations can shift $\Delta G'$ (or A_r) from $\Delta_r G'^{\circ}$ by tens of kJ/mol.

Gibbs free energy quantifies the work available within a system at constant temperature and pressure. eQuilibrator assumes that a temperature of 25°C (298.15 K) and a pressure of 1 bar. $\Delta_r G^{\circ}$ presents the change in Gibbs free energy for a reaction under standard conditions, excluding effects of pH, ionic strength or any other cellular factors (assumed to be zero). $\Delta_r G'^{\circ}$ represents the change in Gibbs free energy at a specific pH and ionic strength. Neither $\Delta_r G^{\circ}$ nor $\Delta_r G'^{\circ}$ accounts for reactant concentration effects on free energy.

To incorporate concentration effects, we decomposed the chemical affinity A_r into the standard chemical potential and a term dependent on the logarithm of the metabolite concentration (in M), as shown in Equation 13. The standard chemical potential reflects the energy state defined by a compound's formation energy—the change in free energy during its formation from elements in their standard state. In eQuilibrator, $\Delta_f G'^{\circ}$ is the formation energy of a compound under specific cellular conditions defined by pH and ionic strength. The default pH is 7 and the default ionic strength is 0.1 M.

For details on how these different values are incorporated into the group contribution method, refer to eQuilibrator and to [NBEF+12]. eQuilibrator also provides free energy values adapted to 1

Figure: Adapted Hynne model

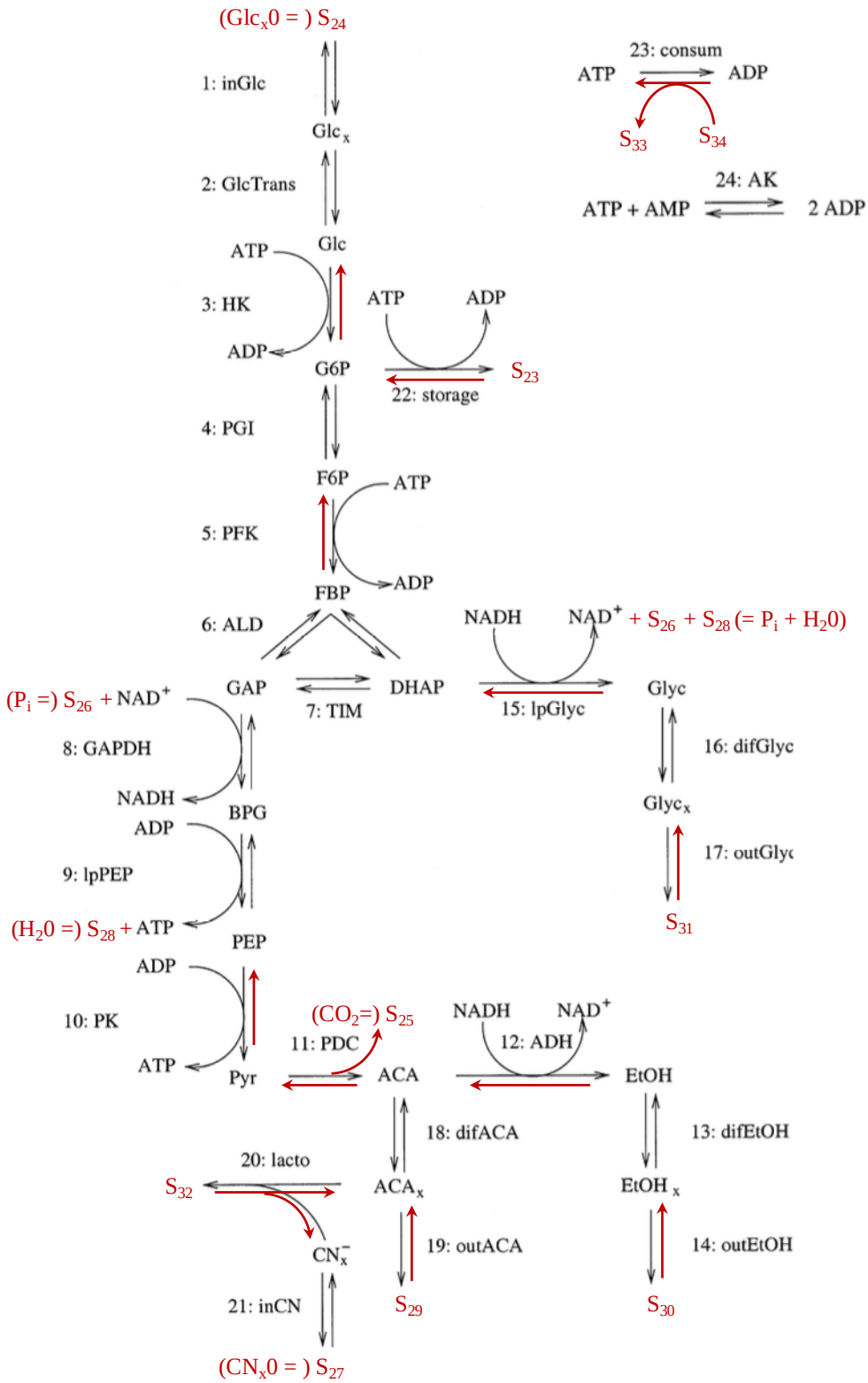

Figure 1: Reaction network of the Hynne model (adapted from [HDS01]). Black arrows, compounds and reaction annotations are original. Red arrows and compounds have been added here for correct reaction balancing.

mM concentration ($\Delta_r G'^m$, $\Delta_f G'^m$), recognizing that this is often more representative of metabolic concentration. While we used Molar units for all concentrations and parameters, using mM would be equally valid.

To parameterize the Hynne model with the TDE kinetics, we used $\Delta_f G'^\circ$ from eQuilibrator at pH 7.5, pMg 3.0, and 0.25 M ionic strength. All values are given in Table 1 for traceability. However, applying these values to a model with realistic concentrations and rates revealed two unit-related problems, discussed below.

4.2 Practical Adjustments Accounting for Concentration and Energy Units

The choice to use $\Delta_f G'^\circ$, i.e. those values determined for standard conditions requires also to adjust all concentration and parameter values of the Hynne model respectively. That means that all concentrations have to be used in M (or practically multiply all unit-less given values in JWS online by 10^{-3}). Equally, all Michaelis-Menten constants, maximal velocities and other rate constants have to be considered, if they contain the unit of concentration.

Another issue is that the value of gas constant multiplied with temperature of about $RT = 2.47897$ J/mol is small compared to many values of standard chemical potentials. Therefore, the practically resulting value of $\frac{M_{\mp r}}{RT}$ needed to calculate the parameter values (e.g. Equation 22) can be in the order of a thousand, potentially resulting in numerical issues, if we want to calculate $e^{\mp\frac{M_{\mp r}}{RT}}$. Since the assignment of all μ^0s of substrates to k_+ and all μ^0s of products to k_- at the transition from Equation 15 to 16 is only determined up to a linear factor (the value β), we can inflict any factor to both kinetic constants without violation of thermodynamic constraints (though change of λ_r). Different choices are possible as long as Equation 15 is fulfilled. We have chosen to subtract the mean of M_{+r} and M_{-r} ($\beta = -(M_{+r} + M_{-r})/2$) from both of them for each reaction. This results in values relatively close to zero, such that the calculation of the exponential function does not create numerical issues.

4.3 Adjustment of the Stoichiometric Matrix N and Addition of Missing Metabolites

The publication of the Hynne model does not provide its stoichiometric matrix **N** directly, but it is evident from the provided set of reactions (their Table 1 and Figure 2). **N** could also be retrieved from the JWS online database. However, we cannot use this matrix directly for a number of reasons.

First, the Hynne model has omitted a number of metabolites that are critical for correct balancing of Gibbs free energies of reactions. Note that we have numbered metabolites included in the Hynne model according to their appearance in tables (see Table 1). Then, we have added the missing metabolites as follows:

- Reaction 11 (PDC) lacks CO_2, added as S_{25}
- Reaction 9 (lpPEP) lacks water, added as S_{28}
- Reaction 8 (GAPDH) lacks orthophosphate, added as S_{26}
- Reaction 15 (lpGlyc) lacks both water and orthophosphate, added as S_{28} and S_{26}

Second, the implementation on JWS online has included the difference in volume between inside the cell and the external medium as a value of 59 in the respective uptake or release reactions, in accordance with chosen value by Hynne et al. We adopted this change, however only for the calculation of concentration changes, not for the calculation of λ_r-values or reaction rates as detailed below.

Third, since our approach considers all reactions as basically reversible, we also added separate metabolites for the sinks of outgoing reactions (there called "P"), i.e.

- Reaction 14 (outEtOH) gets S_{30} as sink
- Reaction 17 (outGlyc) goes to S_{31}
- Reaction 19 (outACA) is supplemented with S_{29}

The concentrations of the added external compounds will still be considered as vanishing and fixed.

Fourth, reactions 22 ("storage") and 23 ("consum") lump many processes consuming glucose-6-phosphate (22) and ATP (22 and 23). Hence, they are also not balanced, which would lead to unrealistic values of Gibbs free energy. In order to adjust the model respectively, we added another product to reaction 22 (S_{23}) and substrate and product to reaction 23 (i.e. S_{33} and S_{34}). In addition, the fixed external species ($Glc_x0 = S_{24}$ and $CN_x0 = S_{27}$) need to be taken into account.

These adjustments lead to two different types of stoichiometric matrices, called here $\mathbf{N}^\lambda$ and $\mathbf{N}^v$ (Equation 6.1 in Appendix). Both matrices contain 24 columns for the reactions considered in the Hynne model. Deviating from the Hynne model, they contain in total 34 rows for all metabolite listed above, i.e. the 22 original metabolites of the Hynne model, as well as the added metabolites to complete the reactions correctly, the sinks for excreted compounds, and the dummy metabolites for lumped processes. $\mathbf{N}^\lambda$ is used, first, to calculate the kinetic constants via its partial stoichiometric matrices and the $\vec{M}$ vector as exemplified in Equations 18 to 22. Here, it reads

$$\vec{M}^\lambda_\pm = \vec{\mu}_0^{\mathrm{T}} \cdot \mathbf{N}^\lambda_\pm \tag{34}$$

Then, the kinetic constants of the r-th reaction read as follows

$$k_{\pm r} = \lambda_r e^{\mp \frac{M^\lambda_{\pm r}}{RT}} \quad \text{for} \quad r = 1, ...R \tag{35}$$

where $M^\lambda_{\pm r}$ is the r-th entry of $\vec{M}^\lambda_\pm$.

Second, the matrix $\mathbf{N}^\lambda$ is used to calculate the rates for all reactions as follows

$$v_r = k_{+r} \prod_{i=1}^{K} S_i^{-N^\lambda_{-i,r}} - k_{-r} \prod_{i=1}^{K} S_i^{N^\lambda_{+i,r}} \quad \text{for} \quad r = 1, ...R \tag{36}$$

where $N^\lambda_{\pm i,r}$ denotes the (i, r)-th entry of the positive or negative partial stoichiometric matrix of $\mathbf{N}^\lambda$, respectively.

The matrix $\mathbf{N}^v$ has two types of modification compared to the matrix $\mathbf{N}^\lambda$. First, all entries in all rows for added metabolites (here in rows 23 to 34) are set to zero to ensure that those metabolites are kept constant in dynamic simulations. Second, matrix $\mathbf{N}^v$ is modified at the entries that reflect transport between different volumes where the respective entries are set to +59 or -59 as in JWSonline. In a general case, these values should reflect the volume ratio between the two compartments that are source or sink for the transport reaction. They should not be confused with stoichiometric coefficients in the sense of numbers of metabolites needing to collide for the reaction to happen. $\mathbf{N}^v$ is used calculate the concentration changes during temporal simulations as in Equation 10.

$$\frac{\mathrm{d}\vec{S}}{\mathrm{d}t} = \mathbf{N}^v \vec{v} \tag{37}$$

Equations 34 to 37 are now the full set of equations required to simulate the dynamic model given the values for the standard chemical potentials and initial concentrations, however, with still unknown parameters λ_r. Next, we discuss how to obtain λ_r-values.

4.4 Determination of Prefactor λ_r

If one intends to formulate a dynamic model for a metabolic network without prior knowledge, λ-values need to be estimated from data for metabolite concentrations and fluxes, as in classical parameter estimation problems. Here, we had the advantage of a fully parameterized model to be used as "ground truth" and, therefore, we used steady state fluxes and concentrations of the Hynne model to derive λ-values for all reactions and then confirmed their suitability by simulating and comparing the dynamic behavior starting with different initial conditions (metabolite concentrations) using either the published or TDE kinetics. Since λ-values should be independent of the specific state (i.e. steady state or not), we rearrange Equations 35 and 36 to yield

$$\lambda_r = \frac{v_{r,ss}}{e^{-\frac{M^\lambda_{-r}}{RT}} \prod_{i=1}^{K} S_{i,ss}^{-N^\lambda_{-i,r}} - e^{+\frac{M^\lambda_{+r}}{RT}} \prod_{i=1}^{K} S_{i,ss}^{N^\lambda_{+i,r}}} \quad \text{for} \quad r = 1, ...R \tag{38}$$

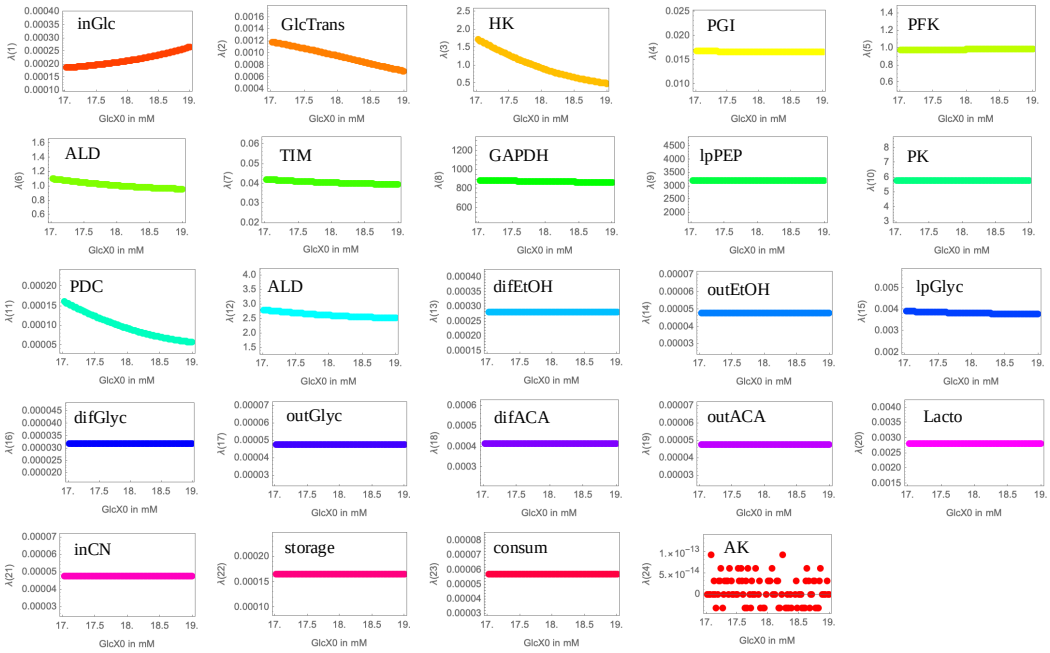

Figure 2: Dependence of λ-values on boundary conditions. To test the effect of boundary conditions, we varied the external glucose concentration Glc_x0 in a range between $17 \cdot 10^{-3}$M and $19 \cdot 10^{-3}$M , recalculated the steady state of the system and resulting λ_r-values. While λ_r-values are constant for most reactions, few reactions show minor dependency.

where $v_{r,ss}$ and $S_{i,ss}$ are reaction rates and metabolite concentrations in steady state, respectively. The resulting values for λ_r-values for all reactions are given in Table 2 in the Appendix.

The λ_r-values that have been calculated based on the steady state assumptions are not completely independent of the chosen boundary conditions affecting the steady state to be reached. In the Hynne model we can, for example, vary the concentration of external glucose (Glc_x0), which leads to different steady states. Hence, also some of the λ_r-values vary slightly as shown in in Fig. 2, however only to minor extent.

Having a deeper look into the properties of λ_r-values, we find that the above calculated values show a tendency to become the larger the more negative the sum of the standard chemical potentials of all substrates and products of a reaction are. To that extend, we have plotted the natural logarithm of λ_r-values against the sum of all standard chemical potentials of substrates and products of the r-the reaction, denoted here with $M_{+r} + M_{-r}$, see Equations 21 and 22 and Figure 3. The linear fit shown is $Log_e[\lambda_r] = -1.4946 - 0.0019426(M_{+r} + M_{-r})$. We did not identify a similar relationship to the difference of M_{+r} and M_{-r}, i.e. the free energy of the reaction. Figuratively speaking, the higher the activation energy of the reaction, i.e. the magnitude of the potential barrier separating minima of the potential energy surface pertaining to the initial and final thermodynamic state, the higher also the respective kinetic parameters, i.e. the λ_r-values. This may indicate that λ_r-values are to some extend dictated by thermodynamic necessities and the cell has to provide catalysts that are respectively strong and abundant.

4.5 Systematic Comparison of TDE Kinetics with Classical Kinetics for Individual Reactions

To analyze the behavior of the kinetics under different conditions, we need a systematic comparison of the TDE kinetics with classical kinetics. Here, we look at all the reactions that are present in the Hynne model. They comprise simple irreversible mass action (e.g. reactions 14, 17, 19, 20, 22, 23), reversible mass action (reactions 1, 9, 13, 16, 18, 21, 24), irreversible and reversible Michaelis-Menten kinetics with different degrees of inhibition (reactions 2-4, 6-8, 10-12, 15) as well as an irreversible

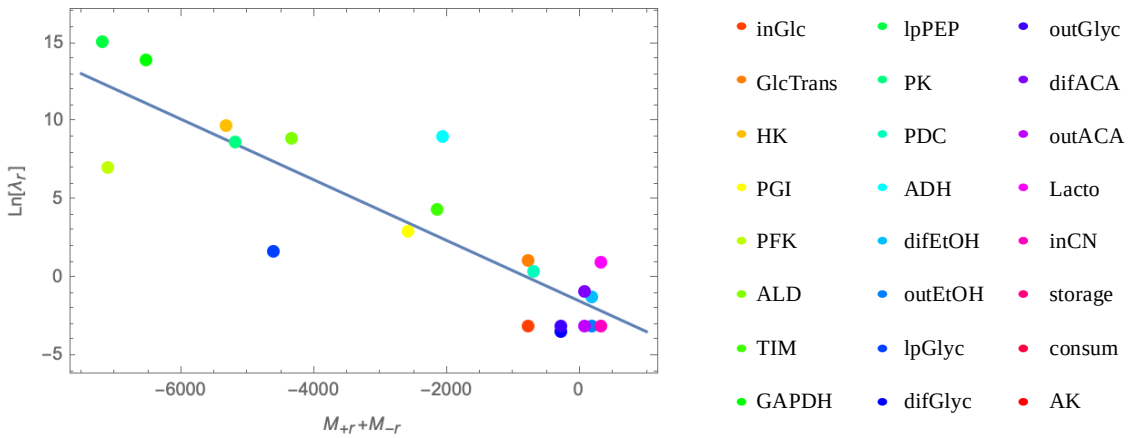

Figure 3: Relation between λ and μ^0 values. The natural logarithm of λ-values is plotted against the sum of all standard chemical potentials of substrates and products of the respective reaction, denoted here with $M_{+r} + M_{-r}$, see Equations 21 and 22. Reactions 22 to 24 have not been included, due to our arbitrary choice of parameters for added substrates. The gray line is a linear fit of data points to guide the eye. Right panel: color code for reactions valid for all figures.

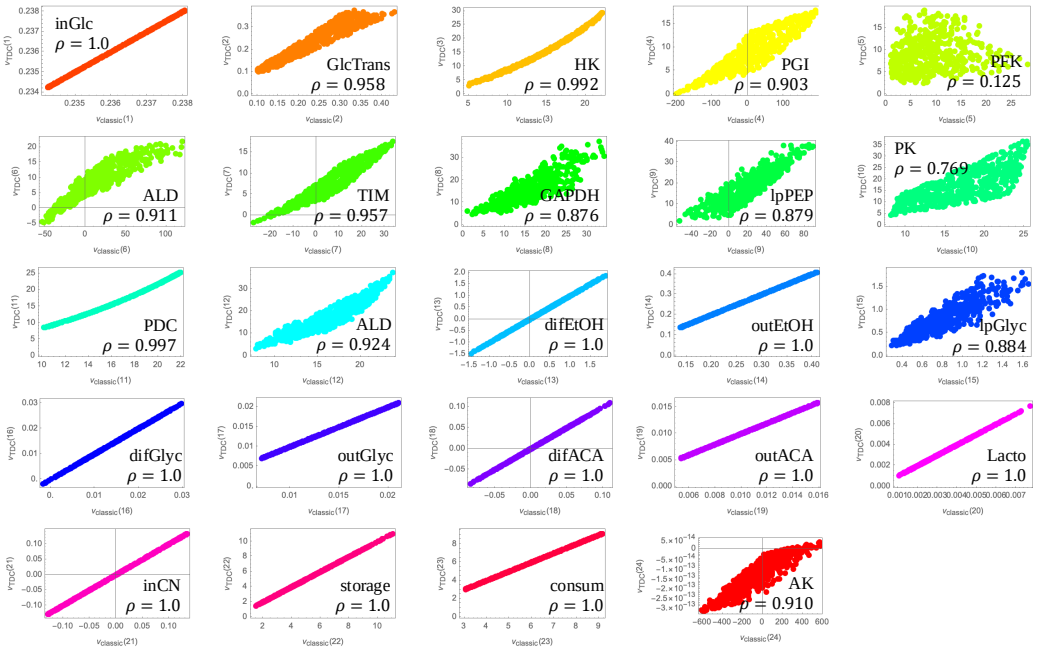

Figure 4: Comparison of classical kinetics to TDE kinetics for individual reactions. We created 1000 sets of metabolite concentrations varied randomly between the 0.5- and 1.5-fold of their steady state value and calculated both the classical rates according to the Hynne model and the TDE rates. Within the panel for each reaction is the correlation coefficient ρ is displayed, which is 1 for reactions with mass action kinetics in the Hynne model and around 0.9 for reactions with Michaelis-Menten kinetics. Only reaction 5 (PFK) with Hill kinetics shows deviating behavior.

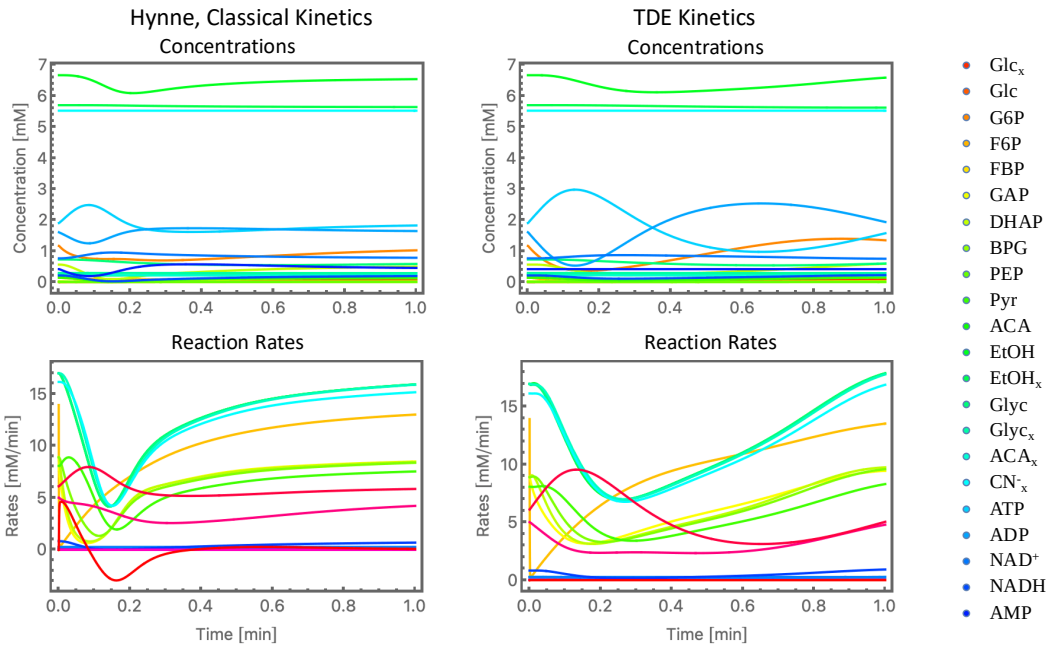

Figure 5: Comparison of model dynamics simulated with either classical kinetics or TDE kinetics. We perturbed the initial concentration of external glucose by setting it to its 0.01-fold compared to the steady state concentration. Left panels: Hynne original kinetics, right panels: TDE kinetics. Top panels: concentration time course, bottom panels: time courses of reaction rates. Right edge: color code for metabolites. Color codes for reactions see Fig. 3.

Hill kinetic (reaction 5). The TDE kinetics instead is in all cases a reversible mass action kinetics. Therefore, it is not self-evident that the behavior should reflect that of classical kinetics. As shown in Fig. 4, we have tested that as follows: we have chosen a steady state with external glucose concentration $Glc_x0 = 5 \cdot 10^{-3}$M and external cyanide concentration $CN_x^-0 = 5.6 \cdot 10^{-3}$M as reference point. For this point, we calculated λ_r as explained above. Then, we sampled the concentration space around the steady state concentration one thousand times choosing each time a new set of random values for the concentrations between their 0.5- and 1.5-fold (uniform distribution). For these sets, we calculated all the rates either with the classical kinetics used by Hynne et al. or with the TDE kinetics. As can be seen in Fig. 4, most rates show comparable values for both approaches; the correlation coefficients are given on top of the panel for each reaction. We see that all reactions that have mass action kinetics at Hynne display a correlation coefficient of 1, thus a replacement has no influence. An exception is reaction 24 which is forced to have zero rate in steady state (because AMP does not enter any other reaction) and therefore leads to numerical uncertainties in determining λ_{24}. Many of the reactions with Michaelis-Menten kinetics at Hynne show correlation coefficients in the order of 0.9 and even above. Given that parameter estimation with real metabolites often very tedious and good fits are hard to achieve, this argues for TDE kinetics as an acceptable replacement. The only clear exception is reaction 5 with a correlation coefficient of only about 0.1. This indicates that the sigmoidal behavior provided by Hill kinetics is not optimally reflected with TDE kinetics, at least not on the level of the individual reaction.

4.6 Simulation Results for Hynne model

With the preparatory steps discussed above, we are ready to simulate the Hynne model. As mentioned above, we simulated both the classical model and our newly parameterized TDE model for a set of example conditions to compare them. As reference point, we have chosen a steady state with external glucose concentration $Glc_x0 = 5 \cdot 10^{-3}$M and external cyanide concentration $CN_x^-0 = 5.6 \cdot 10^{-3}$M. If we start directly at steady state, in both models the system remains in steady state, as required. If we perturb the initial concentrations, here by setting internal glucose to a hundredths of its original value

(i.e. from $Glc_x = 0.0801634 \cdot 10^{-3}$M to $Glc_x = 0.0801634 \cdot 10^{-5}$M, the following dynamic behavior of the TDE model resembles the behavior of the classical model closely as seen in Fig. 5. There are, of course, small deviations, but the qualitative behavior remains.

5 Discussion

We have introduced a thermodynamically explicit (TDE) kinetic approach that utilizes tabulated standard chemical potentials to derive individual kinetic parameters. The method separates the kinetics into a known, chemically determined component (the exponential function containing μ^0) and a biochemically determined component λ-value, which also depends on enzyme amounts and properties. The resulting kinetics is essentially a mass-action kinetics. Comparable approaches have been discussed in the framework of bond graphs (e.g. in [GP22] with an application to photosynthesis) or in [Pfe24] studying toy models to explore the flux solution space. We have demonstrated how the stoichiometric matrix of the metabolic network under study can be used to systematically derive rate equations for the entire network. A key advantage of TDE parametrization is its potential application to metabolic networks of all sizes, from small to genome-scale. Given that eQuilibrator now contains data for approximately 100.000 compounds, providing impressive metabolic coverage, this extensive availability of μ^0-values should facilitate TDE parametrization, particularly for large (potentially genome-wide) metabolic networks.

Basic features of the TDE kinetics have been demonstrated using an accepted and well-studied model of yeast glycolysis introduced by Hynne et al. [HDS01], which employed different types of rate equation from mass action to Michaelis-Menten and Hill equation. To this end, we replaced all the classical kinetics with TDE kinetics, discussed the associated challenges and compared the resulting dynamics and steady state behavior with the original models. The comparison demonstrated that TDE kinetics is not a perfect copy of all classical kinetics, but can provide an easier way to the parametrization of the model. Our work with the Hynne model yielded several important insights. First, accurate balancing of all reaction substrates and products is crucial. Missing metabolites introduce errors in the sum of μ^0-values and can lead to severe numerical issues. Fortunately, current community efforts for quality assurance in genome-scale modeling are strongly supportive to this requirement [LBO+20]. Second, because only the difference of the sum of μ^0-values of substrates and products are relevant, we subtracted their mean from both sums to avoid numerical issues. An alternative approach would be to set one sum to zero and the other to the difference. Third, we treated all reactions as, in principle, reversible. In practice, none of the reactions typically considered irreversible exhibited negative rates, also even in simulations not shown. Fourth, the original Hynne model had been parameterized to exhibit oscillations, a subject of in-depth analysis in their publication. Typical requirements for oscillations in a dynamic system include long-ranging feedback (which we preserved) and non-linear kinetics (which we largely removed). It is important to note that TDE kinetics is less effective at reproducing oscillatory behavior. Therefore, we selected example simulations within a range of boundary conditions that did not exhibit oscillations. Fifth, correct unit handling is essential. We chose to use Molar units for all concentrations and corresponding parameter values. An alternative, particularly using mM, would necessitate using the respective $\Delta_f G'^m$-values provided by eQuilibrator.

Applying the TDE approach to a new model requires parameter estimation, specifically determining the λ_r-values. However, this involves only one parameter per reaction, unlike classical kinetics, which often require multiple parameters (e.g. K_m, V_{max}) A systematic approach would involve performing flux balance analysis to obtain steady state reaction rates, along with a set of steady state metabolite concentrations. Alternatively, time-resolved metabolite concentration data following a defined perturbation could also enable parameter estimation.

For the general case of an unknown prefactor λ, thermodynamically correct parametrization ensures that the resulting rate laws will not violate thermodynamic principles. However, it does not automatically guarantee that the parametrization accurately capture the reaction dynamics. Classical rate laws incorporate features such as dependence on enzyme activity (typically presented by enzyme concentration), saturation effects as well as activation or inhibition by other network components. These effects can be represented by an additional dimensionless prefactor for each affected reaction, as discussed for modular kinetic rate laws [LUK10].

6 Appendices

6.1 Stoichiometric matrices

The stoichiometric matrices for the revised Hynne model read

$$\mathbf{N}^{\lambda} = \begin{bmatrix}
1 & -1 & 0 & 0 & 0 & 0 & 0 & 0 & 0 & 0 & 0 & 0 & 0 & 0 & 0 & 0 & 0 & 0 & 0 & 0 & 0 & 0 & 0 & 0 & 0 \\
0 & 1 & -1 & 0 & 0 & 0 & 0 & 0 & 0 & 0 & 0 & 0 & 0 & 0 & 0 & 0 & 0 & 0 & 0 & 0 & 0 & 0 & 0 & 0 & 0 \\
0 & 0 & 1 & -1 & 0 & 0 & 0 & 0 & 0 & 0 & 0 & 0 & 0 & 0 & 0 & 0 & 0 & 0 & 0 & 0 & 0 & -1 & 0 & 0 \\
0 & 0 & 0 & 1 & -1 & 0 & 0 & 0 & 0 & 0 & 0 & 0 & 0 & 0 & 0 & 0 & 0 & 0 & 0 & 0 & 0 & 0 & 0 & 0 \\
0 & 0 & 0 & 0 & 1 & -1 & 0 & 0 & 0 & 0 & 0 & 0 & 0 & 0 & 0 & 0 & 0 & 0 & 0 & 0 & 0 & 0 & 0 & 0 \\
0 & 0 & 0 & 0 & 0 & 1 & 1 & -1 & 0 & 0 & 0 & 0 & 0 & 0 & 0 & 0 & 0 & 0 & 0 & 0 & 0 & 0 & 0 & 0 \\
0 & 0 & 0 & 0 & 0 & 1 & -1 & 0 & 0 & 0 & 0 & 0 & 0 & 0 & -1 & 0 & 0 & 0 & 0 & 0 & 0 & 0 & 0 & 0 \\
0 & 0 & 0 & 0 & 0 & 0 & 0 & 1 & -1 & 0 & 0 & 0 & 0 & 0 & 0 & 0 & 0 & 0 & 0 & 0 & 0 & 0 & 0 & 0 \\
0 & 0 & 0 & 0 & 0 & 0 & 0 & 0 & 1 & -1 & 0 & 0 & 0 & 0 & 0 & 0 & 0 & 0 & 0 & 0 & 0 & 0 & 0 & 0 \\
0 & 0 & 0 & 0 & 0 & 0 & 0 & 0 & 0 & 1 & -1 & 0 & 0 & 0 & 0 & 0 & 0 & 0 & 0 & 0 & 0 & 0 & 0 & 0 \\
0 & 0 & 0 & 0 & 0 & 0 & 0 & 0 & 0 & 0 & 1 & -1 & 0 & 0 & 0 & 0 & -1 & 0 & 0 & 0 & 0 & 0 & 0 & 0 \\
0 & 0 & 0 & 0 & 0 & 0 & 0 & 0 & 0 & 0 & 0 & 1 & -1 & 0 & 0 & 0 & 0 & 0 & 0 & 0 & 0 & 0 & 0 & 0 \\
0 & 0 & 0 & 0 & 0 & 0 & 0 & 0 & 0 & 0 & 0 & 0 & 1 & -1 & 0 & 0 & 0 & 0 & 0 & 0 & 0 & 0 & 0 & 0 \\
0 & 0 & 0 & 0 & 0 & 0 & 0 & 0 & 0 & 0 & 0 & 0 & 0 & 1 & -1 & 0 & 0 & 0 & 0 & 0 & 0 & 0 & 0 & 0 \\
0 & 0 & 0 & 0 & 0 & 0 & 0 & 0 & 0 & 0 & 0 & 0 & 0 & 0 & 0 & 1 & -1 & 0 & 0 & 0 & 0 & 0 & 0 & 0 \\
0 & 0 & 0 & 0 & 0 & 0 & 0 & 0 & 0 & 0 & 0 & 0 & 0 & 0 & 0 & 0 & 0 & 1 & -1 & -1 & 0 & 0 & 0 & 0 \\
0 & 0 & 0 & 0 & 0 & 0 & 0 & 0 & 0 & 0 & 0 & 0 & 0 & 0 & 0 & 0 & 0 & 0 & 0 & -1 & 1 & 0 & 0 & 0 \\
0 & 0 & -1 & 0 & -1 & 0 & 0 & 0 & 1 & 1 & 0 & 0 & 0 & 0 & 0 & 0 & 0 & 0 & 0 & 0 & 0 & -1 & -1 & -1 \\
0 & 0 & 1 & 0 & 1 & 0 & 0 & 0 & -1 & -1 & 0 & 0 & 0 & 0 & 0 & 0 & 0 & 0 & 0 & 0 & 0 & 1 & 1 & 2 \\
0 & 0 & 0 & 0 & 0 & 0 & 0 & -1 & 0 & 0 & 0 & 1 & 0 & 0 & 1 & 0 & 0 & 0 & 0 & 0 & 0 & 0 & 0 & 0 \\
0 & 0 & 0 & 0 & 0 & 0 & 0 & 1 & 0 & 0 & 0 & -1 & 0 & 0 & -1 & 0 & 0 & 0 & 0 & 0 & 0 & 0 & 0 & 0 \\
0 & 0 & 0 & 0 & 0 & 0 & 0 & 0 & 0 & 0 & 0 & 0 & 0 & 0 & 0 & 0 & 0 & 0 & 0 & 0 & 0 & 0 & 0 & -1 \\
0 & 0 & 0 & 0 & 0 & 0 & 0 & 0 & 0 & 0 & 0 & 0 & 0 & 0 & 0 & 0 & 0 & 0 & 0 & 0 & 0 & 1 & 0 & 0 \\
-1 & 0 & 0 & 0 & 0 & 0 & 0 & 0 & 0 & 0 & 0 & 0 & 0 & 0 & 0 & 0 & 0 & 0 & 0 & 0 & 0 & 0 & 0 & 0 \\
0 & 0 & 0 & 0 & 0 & 0 & 0 & 0 & 0 & 0 & 1 & 0 & 0 & 0 & 0 & 0 & 0 & 0 & 0 & 0 & 0 & 0 & 0 & 0 \\
0 & 0 & 0 & 0 & 0 & 0 & 0 & -1 & 0 & 0 & 0 & 0 & 0 & 0 & 1 & 0 & 0 & 0 & 0 & 0 & 0 & 0 & 0 & 0 \\
0 & 0 & 0 & 0 & 0 & 0 & 0 & 0 & 0 & 0 & 0 & 0 & 0 & 0 & 0 & 0 & 0 & 0 & 0 & 0 & -1 & 0 & 0 & 0 \\
0 & 0 & 0 & 0 & 0 & 0 & 0 & 0 & 1 & 0 & 0 & 0 & 0 & 0 & -1 & 0 & 0 & 0 & 0 & 0 & 0 & 0 & 0 & 0 \\
0 & 0 & 0 & 0 & 0 & 0 & 0 & 0 & 0 & 0 & 0 & 0 & 0 & 0 & 0 & 0 & 0 & 0 & 1 & 0 & 0 & 0 & 0 & 0 \\
0 & 0 & 0 & 0 & 0 & 0 & 0 & 0 & 0 & 0 & 0 & 0 & 0 & 1 & 0 & 0 & 0 & 0 & 0 & 0 & 0 & 0 & 0 & 0 \\
0 & 0 & 0 & 0 & 0 & 0 & 0 & 0 & 0 & 0 & 0 & 0 & 0 & 0 & 0 & 0 & 1 & 0 & 0 & 0 & 0 & 0 & 0 & 0 \\
0 & 0 & 0 & 0 & 0 & 0 & 0 & 0 & 0 & 0 & 0 & 0 & 0 & 0 & 0 & 0 & 0 & 0 & 1 & 0 & 0 & 0 & 0 & 0 \\
0 & 0 & 0 & 0 & 0 & 0 & 0 & 0 & 0 & 0 & 0 & 0 & 0 & 0 & 0 & 0 & 0 & 0 & 0 & 1 & 0 & 0 & 0 & 0 \\
0 & 0 & 0 & 0 & 0 & 0 & 0 & 0 & 0 & 0 & 0 & 0 & 0 & 0 & 0 & 0 & 0 & 0 & 0 & 0 & 0 & 0 & -1 & 0 \\
0 & 0 & 0 & 0 & 0 & 0 & 0 & 0 & 0 & 0 & 0 & 0 & 0 & 0 & 0 & 0 & 0 & 0 & 0 & 0 & 0 & 0 & 1 & 0
\end{bmatrix}$$

$$\mathbf{N}^{\nu} = \begin{bmatrix}
1 & -1 & 0 & 0 & 0 & 0 & 0 & 0 & 0 & 0 & 0 & 0 & 0 & 0 & 0 & 0 & 0 & 0 & 0 & 0 & 0 & 0 & 0 & 0 & 0 \\
0 & 59 & -1 & 0 & 0 & 0 & 0 & 0 & 0 & 0 & 0 & 0 & 0 & 0 & 0 & 0 & 0 & 0 & 0 & 0 & 0 & 0 & 0 & 0 & 0 \\
0 & 0 & 1 & -1 & 0 & 0 & 0 & 0 & 0 & 0 & 0 & 0 & 0 & 0 & 0 & 0 & 0 & 0 & 0 & 0 & 0 & -1 & 0 & 0 \\
0 & 0 & 0 & 1 & -1 & 0 & 0 & 0 & 0 & 0 & 0 & 0 & 0 & 0 & 0 & 0 & 0 & 0 & 0 & 0 & 0 & 0 & 0 & 0 \\
0 & 0 & 0 & 0 & 1 & -1 & 0 & 0 & 0 & 0 & 0 & 0 & 0 & 0 & 0 & 0 & 0 & 0 & 0 & 0 & 0 & 0 & 0 & 0 \\
0 & 0 & 0 & 0 & 0 & 1 & 1 & -1 & 0 & 0 & 0 & 0 & 0 & 0 & 0 & 0 & 0 & 0 & 0 & 0 & 0 & 0 & 0 & 0 \\
0 & 0 & 0 & 0 & 0 & 1 & -1 & 0 & 0 & 0 & 0 & 0 & 0 & 0 & -1 & 0 & 0 & 0 & 0 & 0 & 0 & 0 & 0 & 0 \\
0 & 0 & 0 & 0 & 0 & 0 & 0 & 1 & -1 & 0 & 0 & 0 & 0 & 0 & 0 & 0 & 0 & 0 & 0 & 0 & 0 & 0 & 0 & 0 \\
0 & 0 & 0 & 0 & 0 & 0 & 0 & 0 & 1 & -1 & 0 & 0 & 0 & 0 & 0 & 0 & 0 & 0 & 0 & 0 & 0 & 0 & 0 & 0 \\
0 & 0 & 0 & 0 & 0 & 0 & 0 & 0 & 0 & 1 & -1 & 0 & 0 & 0 & 0 & 0 & 0 & 0 & 0 & 0 & 0 & 0 & 0 & 0 \\
0 & 0 & 0 & 0 & 0 & 0 & 0 & 0 & 0 & 0 & 1 & -1 & 0 & 0 & 0 & 0 & 0 & -59 & 0 & 0 & 0 & 0 & 0 & 0 \\
0 & 0 & 0 & 0 & 0 & 0 & 0 & 0 & 0 & 0 & 0 & 1 & -59 & 0 & 0 & 0 & 0 & 0 & 0 & 0 & 0 & 0 & 0 & 0 \\
0 & 0 & 0 & 0 & 0 & 0 & 0 & 0 & 0 & 0 & 0 & 0 & 1 & -1 & 0 & 0 & 0 & 0 & 0 & 0 & 0 & 0 & 0 & 0 \\
0 & 0 & 0 & 0 & 0 & 0 & 0 & 0 & 0 & 0 & 0 & 0 & 0 & 0 & 1 & -59 & 0 & 0 & 0 & 0 & 0 & 0 & 0 & 0 \\
0 & 0 & 0 & 0 & 0 & 0 & 0 & 0 & 0 & 0 & 0 & 0 & 0 & 0 & 0 & 1 & -1 & 0 & 0 & 0 & 0 & 0 & 0 & 0 \\
0 & 0 & 0 & 0 & 0 & 0 & 0 & 0 & 0 & 0 & 0 & 0 & 0 & 0 & 0 & 0 & 0 & 1 & -1 & -1 & 0 & 0 & 0 & 0 \\
0 & 0 & 0 & 0 & 0 & 0 & 0 & 0 & 0 & 0 & 0 & 0 & 0 & 0 & 0 & 0 & 0 & 0 & 0 & -1 & 1 & 0 & 0 & 0 \\
0 & 0 & -1 & 0 & -1 & 0 & 0 & 0 & 1 & 1 & 0 & 0 & 0 & 0 & 0 & 0 & 0 & 0 & 0 & 0 & 0 & -1 & -1 & -1 \\
0 & 0 & 1 & 0 & 1 & 0 & 0 & 0 & -1 & -1 & 0 & 0 & 0 & 0 & 0 & 0 & 0 & 0 & 0 & 0 & 0 & 1 & 1 & 2 \\
0 & 0 & 0 & 0 & 0 & 0 & 0 & -1 & 0 & 0 & 0 & 1 & 0 & 0 & 1 & 0 & 0 & 0 & 0 & 0 & 0 & 0 & 0 & 0 \\
0 & 0 & 0 & 0 & 0 & 0 & 0 & 1 & 0 & 0 & 0 & -1 & 0 & 0 & -1 & 0 & 0 & 0 & 0 & 0 & 0 & 0 & 0 & 0 \\
0 & 0 & 0 & 0 & 0 & 0 & 0 & 0 & 0 & 0 & 0 & 0 & 0 & 0 & 0 & 0 & 0 & 0 & 0 & 0 & 0 & 0 & 0 & -1 \\
0 & 0 & 0 & 0 & 0 & 0 & 0 & 0 & 0 & 0 & 0 & 0 & 0 & 0 & 0 & 0 & 0 & 0 & 0 & 0 & 0 & 0 & 0 & 0 \\
0 & 0 & 0 & 0 & 0 & 0 & 0 & 0 & 0 & 0 & 0 & 0 & 0 & 0 & 0 & 0 & 0 & 0 & 0 & 0 & 0 & 0 & 0 & 0 \\
0 & 0 & 0 & 0 & 0 & 0 & 0 & 0 & 0 & 0 & 0 & 0 & 0 & 0 & 0 & 0 & 0 & 0 & 0 & 0 & 0 & 0 & 0 & 0 \\
0 & 0 & 0 & 0 & 0 & 0 & 0 & 0 & 0 & 0 & 0 & 0 & 0 & 0 & 0 & 0 & 0 & 0 & 0 & 0 & 0 & 0 & 0 & 0 \\
0 & 0 & 0 & 0 & 0 & 0 & 0 & 0 & 0 & 0 & 0 & 0 & 0 & 0 & 0 & 0 & 0 & 0 & 0 & 0 & 0 & 0 & 0 & 0 \\
0 & 0 & 0 & 0 & 0 & 0 & 0 & 0 & 0 & 0 & 0 & 0 & 0 & 0 & 0 & 0 & 0 & 0 & 0 & 0 & 0 & 0 & 0 & 0 \\
0 & 0 & 0 & 0 & 0 & 0 & 0 & 0 & 0 & 0 & 0 & 0 & 0 & 0 & 0 & 0 & 0 & 0 & 0 & 0 & 0 & 0 & 0 & 0 \\
0 & 0 & 0 & 0 & 0 & 0 & 0 & 0 & 0 & 0 & 0 & 0 & 0 & 0 & 0 & 0 & 0 & 0 & 0 & 0 & 0 & 0 & 0 & 0 \\
0 & 0 & 0 & 0 & 0 & 0 & 0 & 0 & 0 & 0 & 0 & 0 & 0 & 0 & 0 & 0 & 0 & 0 & 0 & 0 & 0 & 0 & 0 & 0 \\
0 & 0 & 0 & 0 & 0 & 0 & 0 & 0 & 0 & 0 & 0 & 0 & 0 & 0 & 0 & 0 & 0 & 0 & 0 & 0 & 0 & 0 & 0 & 0 \\
0 & 0 & 0 & 0 & 0 & 0 & 0 & 0 & 0 & 0 & 0 & 0 & 0 & 0 & 0 & 0 & 0 & 0 & 0 & 0 & 0 & 0 & 0 & 0
\end{bmatrix}$$

6.2 Metabolite and Reaction Information

Relevant numbering and quantitative information about metabolites and reactions in the Hynne model and our extension are provided in the tables below.

Table 1: **Metabolite Information.** Listed are all metabolites originally contained in the Hynne model (S_1 to S_{22}) with their steady state concentrations (for $\text{Glc}_x0 = 5.0 \cdot 10^{-3}$) and their respective standard chemical potentials μ^0 as well as those metabolites added for thermodynamic balancing (S_{23} to S_{34}). Remarks: * μ^0 was arbitrarily set to balance the differences in Gibbs free energy of the missing product. The concentration was set to zero (no re-influx). Note that to prevent numerical issues in Equations 36 and 38, i.e. to prevent 0^0, a small non-zero value can be chosen instead. ** concentrations were set to 1 to mirror their use in the Hynne model (multiplication by 1 does not affect the rate). *** The concentration was set to zero (no re-influx). **** concentrations were set to 1 to mirror their use in the Hynne model. μ^0 was arbitrarily set to balance the differences in Gibbs free energy of the missing substrate and product. For more information see text.

Number	Name	Concentration [M]	μ^0 in [kJ/mol]	Remarks
S_1	Glc_x	$8.01634 \cdot 10^{-5}$	-392.3	
S_2	Glc	$7.29537 \cdot 10^{-6}$	-392.3	
S_3	G6P	$1.16705 \cdot 10^{-3}$	-1287.6	
S_4	F6P	$1.45314 \cdot 10^{-4}$	-1285.0	
S_5	FBP	$1.92354 \cdot 10^{-4}$	-2176.5	
S_6	GAP/G3P	$2.40510 \cdot 10^{-5}$	-1074.4	
S_7	DHAP	$5.63423 \cdot 10^{-4}$	-1080.1	
S_8	BGP/13DPG	$7.11072 \cdot 10^{-8}$	-2194.9	
S_9	PEP	$1.15848 \cdot 10^{-5}$	-1188.0	
S_{10}	Pyr	$1.41006 \cdot 10^{-4}$	-338.1	
S_{11}	ACA	$2.54627 \cdot 10^{-4}$	34.3	
S_{12}	EtOH	$6.67191 \cdot 10^{-3}$	82.4	
S_{13}	EtOH_x	$5.70552 \cdot 10^{-3}$	82.4	
S_{14}	Glyc	$7.30030 \cdot 10^{-4}$	-145.0	
S_{15}	Glyc_x	$2.93243 \cdot 10^{-4}$	-145.0	
S_{16}	ACA_x	$2.21005 \cdot 10^{-4}$	34.3	
S_{17}	CN_x^-	$5.52776 \cdot 10^{-3}$	163.1	
S_{18}	ATP	$1.90052 \cdot 10^{-3}$	-2263.6	
S_{19}	ADP	$1.60722 \cdot 10^{-3}$	-1388.7	
S_{20}	NAD^+	$7.65889 \cdot 10^{-4}$	-1128.9	
S_{21}	NADH	$2.14111 \cdot 10^{-4}$	-1062.7	
S_{22}	AMP	$4.17601 \cdot 10^{-4}$	-514.2	
S_{23}	product of reaction 22	0	-2210.0	μ^0 and concentration set*
S_{24}	Glc_x0	$5.0 \cdot 10^{-3}$	-392.3	determines steady state
S_{25}	CO_2	1	-394.4	concentration set**
S_{26}	P_i	1	-1055.5	concentration set**
S_{27}	CN_x^-	$5.6 \cdot 10^{-5}$	163.1	determines steady state
S_{28}	H_2O	1	-150.9	concentration set**
S_{29}	P, sink for ACA_x	0	34.3	concentration set***
S_{30}	P, sink for EtOH_x	0	82.4	concentration set***
S_{31}	P, sink for Glyc_x	0	-145.0	concentration set***
S_{32}	P, sink for Glyc_x, ACA_x	0	160.0	concentration set***
S_{33}	substrate of reaction 24	1	0	μ^0 and concentration set****
S_{34}	product of reaction 24	1	-895.0	μ^0 and concentration set****

Table 2: **Reaction Information.** Listed are all reactions of the model with their steady state rates and the respective λ-values. The unit of λ-values is dependent on the number of reactants and can vary between min^{-1} for one reactant, $\text{M}^{-1}\ \text{min}^{-1}$ for two reactants, and $\text{M}^{-2}\ \text{min}^{-1}$ for three reactants.

Number	Name	Rate in [M/min]	λ
r_1	inGlc_x	$2.36152 \cdot 10^{-1}$	$4.79999 \cdot 10^{-2}$
r_2	GlcTrans	$2.36152 \cdot 10^{-1}$	$3.24082 \cdot 10^{0}$
r_3	HK	$1.3933 \cdot 10^{1}$	$1.74539 \cdot 10^{4}$
r_4	PGI	$8.90949 \cdot 10^{0}$	$1.98736 \cdot 10^{1}$
r_5	PFK	$8.90949 \cdot 10^{0}$	$1.15641 \cdot 10^{3}$
r_6	ALD	$8.90949 \cdot 10^{0}$	$7.28263 \cdot 10^{3}$
r_7	TIM	$8.07902 \cdot 10^{0}$	$7.74354 \cdot 10^{1}$
r_8	GAPDH	$1.69885 \cdot 10^{1}$	$1.17463 \cdot 10^{6}$
r_9	lpPEP	$1.69885 \cdot 10^{1}$	$3.73279 \cdot 10^{6}$
r_{10}	PK	$1.69885 \cdot 10^{1}$	$6.08244 \cdot 10^{3}$
r_{11}	PDC	$1.69885 \cdot 10^{1}$	$1.46490 \cdot 10^{0}$
r_{12}	ADH	$1.61580 \cdot 10^{1}$	$8.43053 \cdot 10^{3}$
r_{13}	difEtOH	$2.73865 \cdot 10^{-1}$	$2.83389 \cdot 10^{-1}$
r_{14}	outEtOH	$2.73865 \cdot 10^{-1}$	$4.80000 \cdot 10^{-2}$
r_{15}	lpGlyc	$8.30465 \cdot 10^{-1}$	$5.36985 \cdot 10^{0}$
r_{16}	difGlyc	$1.40757 \cdot 10^{-2}$	$3.22034 \cdot 10^{-2}$
r_{17}	outGlyc	$1.40757 \cdot 10^{-2}$	$4.80000 \cdot 10^{-2}$
r_{18}	difACA	$1.40757 \cdot 10^{-2}$	$4.18645 \cdot 10^{-1}$
r_{19}	outACA	$1.06083 \cdot 10^{-2}$	$4.80000 \cdot 10^{-2}$
r_{20}	lacto	$3.46743 \cdot 10^{-3}$	$2.83828 \cdot 10^{0}$
r_{21}	inCN	$3.46743 \cdot 10^{-3}$	$4.79985 \cdot 10^{-2}$
r_{22}	storage	$5.02349 \cdot 10^{0}$	$1.65515 \cdot 10^{-1}$
r_{23}	consum	$6.11107 \cdot 10^{0}$	$5.70793 \cdot 10^{-2}$
r_{24}	AK	$-5.68434 \cdot 10^{-14}$	$5.50674 \cdot 10^{-11}$

References

[Alb94] Robert A Alberty. Biochemical thermodynamics. *Biochimica et Biophysica Acta (BBA)-Protein Structure and Molecular Enzymology*, 1207(1):1–11, 1994.

[Alb03] Robert A Alberty. *Thermodynamics of biochemical reactions*. John Wiley & Sons, 2003.

[BGM+22] Moritz E Beber, Mattia G Gollub, Dana Mozaffari, Kevin M Shebek, Avi I Flamholz, Ron Milo, and Elad Noor. equilibrator 3.0: a database solution for thermodynamic constant estimation. *Nucleic acids research*, 50(D1):D603–D609, 2022.

[GP22] Peter J Gawthrop and Michael Pan. Network thermodynamics of biological systems: A bond graph approach. *Mathematical Biosciences*, 352:108899, 2022.

[GW67] Cato Maximilian Guldberg and Peter Waage. *Etudes sur les affinités chimiques*. Brøgger & Christie, 1867.

[HDS01] Finn Hynne, Sune Danø, and Preben G Sørensen. Full-scale model of glycolysis in saccharomyces cerevisiae. *Biophysical chemistry*, 94(1-2):121–163, 2001.

[LBO+20] Christian Lieven, Moritz E Beber, Brett G Olivier, Frank T Bergmann, Meric Ataman, Parizad Babaei, Jennifer A Bartell, Lars M Blank, Siddharth Chauhan, Kevin Correia, et al. Memote for standardized genome-scale metabolic model testing. *Nature biotechnology*, 38(3):272–276, 2020.

[LK06] Wolfram Liebermeister and Edda Klipp. Bringing metabolic networks to life: convenience rate law and thermodynamic constraints. *Theoretical Biology and Medical Modelling*, 3:1–13, 2006.

[LUK10] Wolfram Liebermeister, Jannis Uhlendorf, and Edda Klipp. Modular rate laws for enzymatic reactions: thermodynamics, elasticities and implementation. *Bioinformatics*, 26(12):1528–1534, 2010.

[Mav91] Michael L Mavrovouniotis. Estimation of standard gibbs energy changes of biotransformations. *Journal of Biological Chemistry*, 266(22):14440–14445, 1991.

[MM+13] Leonor Michaelis, Maud L Menten, et al. Die kinetik der invertinwirkung. *Biochem. z*, 49(333-369):352, 1913.

[NBEF+12] Elad Noor, Arren Bar-Even, Avi Flamholz, Yaniv Lubling, Dan Davidi, and Ron Milo. An integrated open framework for thermodynamics of reactions that combines accuracy and coverage. *Bioinformatics*, 28(15):2037–2044, 2012.

[NHMF13] Elad Noor, Hulda S Haraldsdóttir, Ron Milo, and Ronan MT Fleming. Consistent estimation of gibbs energy using component contributions. *PLoS computational biology*, 9(7):e1003098, 2013.

[PEVN+17] Martin Peters, Johann J Eicher, David D Van Niekerk, Dagmar Waltemath, and Jacky L Snoep. The jws online simulation database. *Bioinformatics*, 33(10):1589–1590, 2017.

[Pfe24] Benjamin Pfeuty. Free-energy transduction mechanisms shape the flux space of metabolic networks. *Biophysical Journal*, 123(20):3600–3611, 2024.

[WG64] P Waage and CM Guldberg. Studier over affiniteten. *Forhandlinger i Videnskabs-selskabet i Christiania*, 1:35–45, 1864.